

Blink-Suppressed Hand Redirection

André Zenner*

Kora Persephone Regitz†

Antonio Krüger‡

Saarland University & German Research Center for Artificial Intelligence (DFKI)
Saarland Informatics Campus, Saarbrücken, Germany

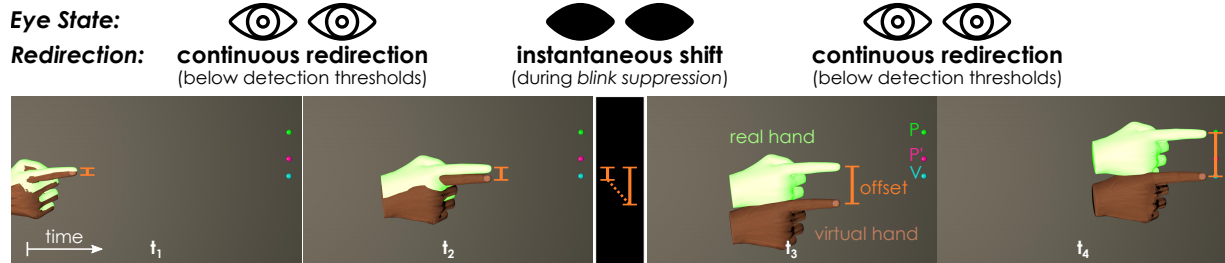


Figure 1: We introduce *Blink-Suppressed Hand Redirection* (BSHR), a novel body warping technique that leverages the temporary blindness of users during blinks. The technique we propose continuously increases the real-to-virtual hand offset only below detection thresholds when the user’s eyes are opened (from t_1 to t_2 , and from t_3 to t_4), and instantaneously adds additional offset during moments of blink-induced visual suppression (from t_2 to t_3). In a psychophysical experiment, we examine the amount of hand redirection that can go unnoticed with this approach and compare it to a current state-of-the-art technique.

ABSTRACT

Many interaction techniques in virtual reality break with the 1-to-1 mapping from real to virtual space. Instead, specialized techniques for 3D interaction and haptic retargeting leverage hand redirection, offsetting the virtual hand rendering from the real hand position. To achieve unnoticeable hand redirection, however, the utilization of change blindness phenomena has not been systematically explored. Inspired by recent advances in the domain of redirected walking, we present the first hand redirection technique that makes use of blink-induced visual suppression and corresponding change blindness. We introduce *Blink-Suppressed Hand Redirection* (BSHR) to study the feasibility and detectability of hand redirection based on blink suppression. Our technique is based on Cheng et al.’s (2017) [9] body warping algorithm and instantaneously shifts the virtual hand when the user’s vision is suppressed during a blink. Additionally, it can be configured to continuously increment hand offsets when the user’s eyes are opened, limited to an extent below detection thresholds. In a psychophysical experiment, we verify that unnoticeable blink-suppressed hand redirection is possible even in worst-case scenarios, and derive the corresponding conservative detection thresholds (CDTs). Moreover, our results show that the range of unnoticeable redirection can be increased by combining continuous warping and blink-suppressed instantaneous shifts. As an additional contribution, we derive the CDTs for Cheng et al.’s (2017) [9] redirection technique that does not leverage blinks.

Keywords: Virtual reality, hand redirection, haptic retargeting, blink suppression, detection thresholds.

Index Terms: H.5.1 [Information Interfaces and Presentation]: Multimedia Information Systems—Artificial, augmented, and virtual realities; H.5.2 [Information Interfaces and Presentation]: User Interfaces—Evaluation/methodology, Interaction styles

*e-mail: andre.zenner@dfki.de

†e-mail: kora.regitz@dfki.de

‡e-mail: krueger@dfki.de

1 INTRODUCTION

As virtual reality (VR) applications are becoming increasingly interactive, the integration of our most natural interfaces to the surrounding world – our hands – has become a central aspect of intuitive VR. While hand tracking solutions allow capturing the position and orientation of the user’s hands and fingers in real time, some interaction techniques break with the 1-to-1 mapping of real and virtual hands. Hand retargeting techniques, for example, make use of intentional displacements of the virtual hand rendering. Techniques such as body warping [3] thereby leverage the visual dominance of human perception to control the trajectory of real hand movements.

Hand redirection (HR) approaches have gained increasing attention from the research community lately, with techniques being proposed for realizing 3D interaction techniques [39], haptic retargeting [2, 3, 9], redirected touching [29, 45], or ergonomic interactions [34]. Approaches studied by researchers offset the virtual hand of a user either by a constant amount (e.g. [4, 21]), or incrementally as the user moves their hands (e.g. [3, 9, 15, 21, 29, 58]). Conceptually, HR is closely related to *redirected walking* (RDW) [40]. RDW solves a related problem and redirects the user’s real walking path while exploring immersive virtual environments (IVEs) on foot. Also here, manipulations of the real-to-virtual mapping are employed, but usually applied to the user’s view instead of the hands.

Past research on RDW examined how perceptual phenomena such as *change blindness* can be utilized to improve redirection. Change blindness describes “the inability to detect changes to an object or scene” [43], and has been leveraged in a variety of ways to enhance VR experiences. Previous work, for example, hid changes to a virtual scene from the user’s attention by applying manipulations when they were out of the user’s sight [49], while the user was temporarily blind during blinks [30, 35] or saccades [51], and even when changes occurred within the user’s field of view (FOV) but outside the visual attention area [33]. In the field of hand redirection research, however, the potential of utilizing change blindness effects has not yet been systematically considered.

In this paper, we transfer the concept of leveraging change blindness to hand redirection and, to the best of our knowledge, propose the first body warping technique that makes use of blink suppression. Our contributions can be summarized as follows:

1. We propose *Blink-Suppressed Hand Redirection* (BSHR), the

first proof-of-concept body warping technique designed to showcase the feasibility, and to enable the investigation, of the concept of leveraging blink suppression for HR. BSHR is based on the body warping technique by Cheng et al. [9].

2. We verify that unnoticeable blink-suppressed hand redirection is possible with our proposed approach. For this, we derive the respective conservative detection thresholds (CDTs) along three different directions. Our results find the ranges of unnoticeable blink-suppressed hand redirection along each direction to be significantly greater than 0cm and of the same order of magnitude as the CDTs of conventional approaches.
3. We derive estimations for the CDTs of Cheng et al.'s [9] original body warping technique along the same directions.
4. We show that when displacing the virtual hand horizontally (right) or vertically (down), combining blink-suppressed hand redirection with incremental warping increases the range of hand redirection that goes unnoticed, compared to utilizing blink-suppressed hand redirection only.

In the following, we briefly review related work on hand redirection, change blindness, and eye blinks. We then introduce the conceptual idea of *Blink-Suppressed Hand Redirection*, along with the assumptions it is based on, and our implementation. The paper then presents our psychophysical evaluation and concludes with a critical discussion of our findings and implications for future work.

2 RELATED WORK

This section reviews related research in the fields of VR hand redirection, change blindness techniques, and human eye blinks.

2.1 Hand Redirection in Virtual Reality

Hand redirection (HR) refers to a controlled manipulation of the real-to-virtual mapping. The goal of HR, as studied here, is to grant the VR system control over the user's real hand movement by *redirecting* the hand towards an alternative target. Similar to how RDW tricks users into walking a physical path in reality that is different from the virtual path traversed in VR [40], HR techniques lead the real hands of a user to follow a trajectory different from what the user sees and assumes to be following [29].

Redirection of the hands is of value in many VR application areas. Most prominently, the technique has been used to enhance the scalability of passive haptic feedback [22, 23]. Kohli [29] introduced the idea of *redirected touching* and used distortions in a virtual scene in combination with HR to convey the perception of differently shaped virtual objects utilizing only a single haptic proxy. Azmandian et al. [3] later proposed to use HR for the realization of *haptic retargeting*. In an illustrative proof of concept, the authors let users interact with a set of spatially dislocated virtual cubes that were all mapped to a single physical proxy. Users could seamlessly interact with the virtual objects as the system redirected their hands to the single proxy in the real environment. Cheng et al. [9] later proposed an extension of the technique introduced by Azmandian et al. [3]. Abtahi and Follmer [1] employed HR to enhance the perceived resolution and speed of shape displays. Later, Abtahi et al. [2] and Gonzalez et al. [19] made use of the technique also in encountered-type haptic systems to account for spatial and temporal limitations of robotic proxies. Zenner and Krüger recently proposed to combine HR with the concept of dynamic passive haptic proxies to extend their range of haptic effects [57, 59]. Besides haptic retargeting, non-isomorphic mappings of the real and virtual hands have also been proposed in the context of 3D interaction techniques such as the Go-Go technique [39]. Moreover, systems that convey pseudo-haptic effects make use of real-to-virtual hand offsets, typically by modifying the control/display ratio to simulate the sensation of drag or weight [13, 24, 41, 42]. Subtle redirection of the user's hands can also help make interactions with virtual user interfaces and scenes more ergonomic, as has been shown by the research of

Murillo et al. [34]. Furthermore, the interaction with tools in VR can benefit from redirection [47, 56].

HR techniques, also referred to as *body warping*, leverage the phenomenon of visual dominance [18]. When visual and proprioceptive sensations are in conflict, i.e. where we *see* our hands is different from where we *feel* our hands to be, the brain tends to trust visual information more, which leads us to perceive our hand to be at the location where it is displayed in VR. As a consequence, when reaching for a target in VR, HR techniques can offset the virtual hand rendering in one direction to trigger a compensatory movement of the real hand in the opposite direction. Previous research introduced a set of techniques for hand warping, either applying constant offsets (e.g. [4, 21]), or continuously increasing the offset as the user moves the hand (e.g. [3, 8, 9, 15, 29, 45, 58, 60]). Ogawa et al. [37] found realistic avatars to decrease hand remapping noticeability. Moreover, researchers derived detection thresholds for HR, for example, in worst-case redirection scenarios [58], or when bimanual redirection is applied [20], a haptic cue is present at the hand during redirection [1], hand movements are scaled [15], hand offsets are constant [4], or users are simultaneously playing a game [8]. Existing HR algorithms, however, do not yet make use of potential change blindness effects, which have already proven themselves as highly useful in related domains such as for RDW.

2.2 Leveraging Change Blindness

With VR being a human-computer interface that grounds itself on a heavy use of sensory stimulation [25], researchers in the past have often tried to make use of perceptual illusions and phenomena. One example of this is the use of *change blindness illusions*. Steinicke et al. [46] introduced such techniques that covertly alter virtual scenes in stereoscopic projection systems. Lately, change blindness has been actively explored in the field of RDW [36]. Suma et al. introduced the technique of *change blindness redirection* [48, 49] to allow users to explore virtual scenes on foot that are much larger than the physically available walking space. With *impossible spaces*, change blindness redirection was further extended to compress large IVEs into confined real walking areas [50]. Change blindness redirection grounds itself on the inability of users to notice changes in the IVE, for example the re-positioning of a door or walls in a virtual room, when they happen outside their field of view (FOV). Such changes in a scene can be triggered, for example, when users look away [49].

Looking away, however, is not the only opportunity for change blindness techniques to inject changes in a scene. Other opportunities include, for example, moments in which the user *focuses* on other parts of the IVE. Marwecki et al. [33] recently explored how changes to a scene outside the user's area of attention but still inside the FOV can be applied without users noticing them. However, tracking the user's attention adds complexity to solutions leveraging change blindness. Thus, other techniques take advantage of recurring moments of visual suppression. During eye blinks, i.e. when the user quickly closes and opens their eyelids, and saccades, i.e. during the short ballistic eye movements in between fixations, the visual perception of users is largely suppressed, which leads to users temporarily being (almost) blind [54]. Langbehn et al. [30] as well as Nguyen and Kunz [35] studied how blink suppression can be utilized to enhance RDW by rotating or translating the scene when the user's eyes are closed. Further research by Bolte and Lappe [5], as well as Sun et al. [51], additionally examined how saccadic suppression (occurring more frequently, but being shorter in time) can likewise be of value for RDW. Motivated by these promising results [30, 35], we investigate how change blindness as a result of blink suppression can be taken advantage of to realize HR.

2.3 Human Eye Blinks

Eye blinks, i.e. the quick down-up movement of the eyelids, protect our eyes and lubricate the cornea [17]. Humans typically blink 10

to 20 times per minute [14, 31] and previous research found the blink frequency to drop when using computer monitors [38]. Recent results by Dennison et al. [12], however, indicate that the use of head-mounted displays (HMDs) increases blink frequencies compared to computer monitors, which motivates research on VR techniques utilizing blink-induced suppression [30]. Blinks can be either voluntary (e.g. in the context of social interaction), spontaneous (i.e. periodically occurring without external stimuli [17]), a reflex (i.e. initiated by bright light or objects that approach rapidly [17]), or externally triggered [11, 53]. During a blink, the eyelid occludes the pupil, which hinders light from entering the eye and consequently reduces retinal illumination for $100ms - 150ms$ [54]. Besides this mechanical interruption of vision, active visual suppression in the brain begins shortly before blink onset and lasts for $100ms - 200ms$ [54]. Bristow et al. [6] found indication of a neural suppression mechanism triggered during blinks. This mechanism affects specific parietal and prefrontal brain regions, and is potentially responsible for the reduction of visual input during blinks usually going unnoticed.

From the perspective of VR research, blinks seem to be suitable opportunities to covertly manipulate the IVE. Being (1) reliably and easily tracked with off-the-shelf eye tracking solutions, (2) periodically occurring, (3) relatively long (compared to the avg. duration of saccades of only $50ms$ [54]), and (4) triggerable through external stimuli, blinks lend themselves to being used for enhancing VR hand redirection. In the following, we present a technique that makes use of the change blindness occurring as a result of blink suppression. With this technique, we study the range in which unnoticeable blink-suppressed hand redirection in VR is possible.

3 BLINK-SUPPRESSED HAND REDIRECTION

The algorithm we outline in the following is, to the best of our knowledge, the first to leverage change blindness during blink suppression for hand redirection. When designing the algorithm, our aim was to develop a proof-of-concept technique that allows us to study the perceptibility of blink-suppressed HR. To this end, we aimed for an approach that supports two modes of redirection: (*Mode 1*) *pure* blink-suppressed redirection, which means that hand offsets are *only* introduced during blinks, and (*Mode 2*) *combined* redirection, which means that offsets are introduced *before, during and after* a blink.

3.1 Concept

We base our algorithm for *Blink-Suppressed Hand Redirection* (BSHR) on the body warping approach of Cheng et al. [9]. Fig. 1 shows an illustration. BSHR redirects the user starting at an origin location O so that the virtual hand arrives at a virtual target V while the physical hand is redirected to reach a physical target P simultaneously. The introduction of real-to-virtual hand offset in the proposed BSHR algorithm is governed by two central ideas:

1. While the user's eyes are *open* and the user reaches for the target, BSHR *continuously* increases the offset of the virtual to the real hand as in the original algorithm by Cheng et al. [9], but *only within ranges that go unnoticed (defined as a parameter)*.
2. When the user *closes* their eyes, i.e. during blink suppression, BSHR *instantaneously* changes the hand offset in a way that, after being compensated for, allows reaching the target by continuing to apply only unnoticeable warping as in step 1.

To implement this behavior, BSHR redirects the physical hand continuously towards a dummy location P' , the computation of which will be introduced in Sect. 3.3. This dummy location still lies within the range of unnoticeable continuous redirection, which ensures that while the user's eyes are open, only an unnoticeable amount of warping is applied. The additional offset required to reach the target P , but not achievable within unnoticeability ranges, is added during a moment of visual suppression, i.e. when the user blinks. This approach of introducing instantaneous, translational shifts is motivated by results of Han et al. [21] and Benda et al. [4],

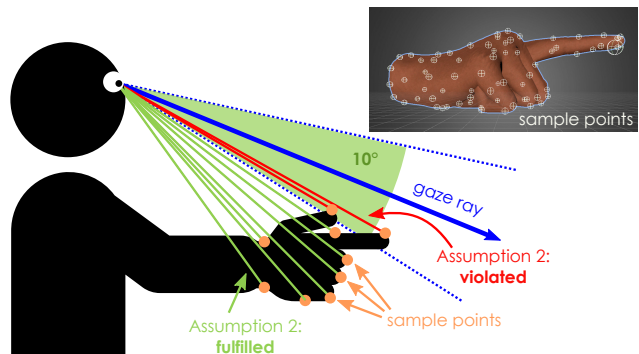


Figure 2: The check for assumption 2. It is checked, for each sample point on the virtual hand model and each sample translated by \vec{b} , if its position is within the user's 10° focus area around the gaze ray. The upper right image depicts our distribution of samples.

which evaluated the use of fixed positional hand offsets. Their studies, while not adding such offsets during blink suppression, revealed detection thresholds of practical relevance [4] and found translational shift to outperform their interpolated reach technique [21].

3.1.1 Reducing the Noticeability of Continuous Warping

To minimize the risk of incremental warping being detected while the user's eyes are open, BSHR only applies continuous redirection below detection thresholds. As thresholds can vary with reaching distance and other interaction aspects [1, 8, 15, 20, 58], we leave them free as an input to the BSHR algorithm. In our work, we employ the worst-case CDT estimates of Zenner and Krüger [58] for desktop-scale redirection as the algorithm's internal representation of the unnoticeability range. This *unnoticeability range* encompasses all real positions around V reachable with the real hand without exceeding any of the detection thresholds for either (1) redirection *angle* (β_{max}) or (2) *minimum* (g_{min}) or (3) *maximum* (g_{max}) *gain*. To realize pure blink-suppressed redirection (*Mode 1*), it suffices to reduce the unnoticeability range to a size of 0 (i.e. $\beta_{max} = 0; g_{min} = g_{max} = 1$); larger ranges result in combined redirection (*Mode 2*). Fig. 3 illustrates the unnoticeability range in 2D.

3.1.2 Reducing the Noticeability of Instantaneous Warping

Inspired by the work of Marwecki et al. [33] and illustrated in Fig. 2, we also added a mechanism to reduce the noticeability of instantaneous hand shifts during blinks. This mechanism prevents BSHR from injecting hand offsets if the virtual hand rendering is likely to jump from outside to inside the user's visual focus area, or vice versa. For this, a subroutine checks where the virtual hand is rendered when the user closes their eyes, and then approximates where it would be rendered if the offset was changed during the blink. Only if neither of these two rendering locations intersect the user's visual focus, the hand offset actually changes during the blink.

3.2 Assumptions

The introduced measures, and our general concept, lead to three assumptions our proof-of-concept algorithm is based on:

- **Assumption 1:** the user blinks ≥ 1 times while reaching for the target.
- **Assumption 2:** the rendering of the virtual hand of the user does not intersect the user's visual focus area before and after the hand offset is changed during a blink (approximated here as everything $\leq 10^\circ$ from the gaze ray, representing the 5° foveal vision area [33] and additional 5° eye tracking tolerance).
- **Assumption 3:** continuous angular hand warping up to β_{max} , and gain-based hand warping g with $g_{min} \leq g \leq g_{max}$, are

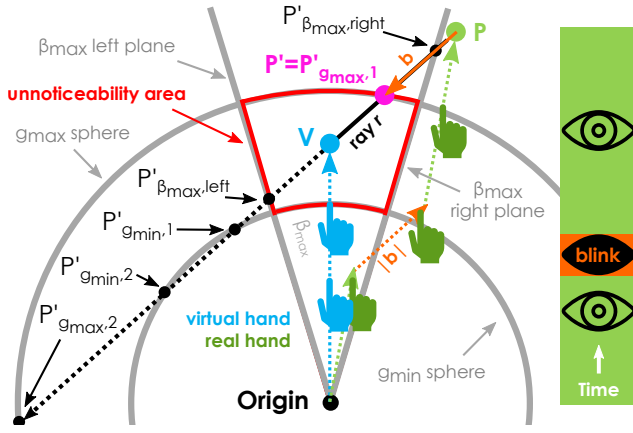


Figure 3: Orthogonal top-down view of the BSHR approach incl. V , P , P' , the unnoticeability area, central vectors, and intersection points. While the offset vector \vec{b} is added to the virtual hand during a blink, for simplicity, we sketch here the respective trajectory of the real hand assuming perfect compensation for hand offsets.

below detection thresholds and likely to go unnoticed by users¹.

We assume: $\beta_{max} = 4.5^\circ$; $g_{min} = \frac{real}{virtual} = 0.94$; $g_{max} = 1.14$ based on related work [58].

In our evaluation, we ensured that assumptions 1 and 2 were met by only considering trials that fulfilled both conditions. Assumption 3 is indirectly built into the algorithm's computation of P' .

3.3 Algorithm

Algorithm 1 shows the pseudocode of BSHR. When starting a new redirection, the algorithm is initialized by the *INIT* procedure. The *UPDATE* function is called every frame to re-compute the virtual hand position H_v . Extending Cheng et al.'s [9] approach, this computation determines a warp vector \vec{W} , representing the offset of the virtual hand from the real hand at position H_p :

$$H_v = H_p + \vec{W} \quad (1)$$

The BSHR algorithm re-computes this warp vector frame-wise as:

$$\vec{W} = \alpha \cdot (V - P') + \vec{b} \quad (2)$$

where

$$\alpha = \frac{|(H_p + \vec{b}) - O|}{|(H_p + \vec{b}) - O| + |(H_p + \vec{b}) - P'|} \quad (3)$$

and

$$\vec{b} = \begin{cases} \vec{0}, & \text{before the 1st valid blink} \\ P' - P, & \text{else} \end{cases} \quad (4)$$

These equations represent a redirection as in Cheng et al. [9]'s original algorithm, with the difference that the real hand is *continuously* redirected towards a dummy location P' (instead of P), and the remaining distance from P to P' is *instantaneously* added to the hand offset as a constant offset vector \vec{b} during the first valid blink (see Equation 4 and line 8–10 in Algorithm 1).

3.3.1 Determining a Valid Blink

The occurrence of the first valid blink is determined using eye tracking data, i.e. querying (1) if the eyes are closed, and (2) the eye gaze

¹We would like to note that past research only considered the detectability of redirection along single dimensions (e.g. only horizontal, vertical or depth-based warping) [58]. For simplicity, to support any direction, and due to a lack of alternative results, BSHR assumes offsets also go unnoticed within the naïve combination of these single-dimension thresholds in this paper.

Algorithm 1 Blink-Suppressed Hand Redirection

Input: Locations: origin O , real target P , virtual target V ;
 Unnoticeability Range: detection thresholds β_{max} , g_{min} , g_{max} ;
 Frame-Wise: real hand position H_p , eye tracking data $eyes$.

Output: virtual hand position H_v

```

1: procedure INIT( $O, P, V, \beta_{max}, g_{min}, g_{max}$ )
2:    $P' \leftarrow$  ComputeDummyTarget( $O, P, V, \beta_{max}, g_{min}, g_{max}$ )
3:    $\vec{b} \leftarrow \vec{0}$ 
4: end procedure
5:
6: procedure UPDATE( $H_p, eyes$ )
7:   // check for valid blink
8:   if  $eyes_{closed}$  && Assumption2( $H_p, \vec{b}, eyes_{gaze}$ ) then
9:      $\vec{b} \leftarrow P' - P$ 
10:  end if
11:  // warp hand
12:   $\alpha = \frac{|(H_p + \vec{b}) - O|}{|(H_p + \vec{b}) - O| + |(H_p + \vec{b}) - P'|}$ 
13:   $\vec{W} = \alpha \cdot (V - P') + \vec{b}$ 
14:   $H_v = H_p + \vec{W}$ 
15: end procedure

```

ray. To check for assumption 2, the model of the virtual hand was populated with 68 invisible reference positions distributed over the surface of the hand as shown in Fig. 2. To determine if the model was visible in the user's visual focus, the angles of the gaze vector and the vector from gaze ray origin towards each reference position were checked against a threshold of 10° according to assumption 2. The same checks were also conducted for each reference position translated by \vec{b} to approximate the hand location after the blink.

3.3.2 Computation of P'

The computation of P' constitutes a central part of the BSHR algorithm. The dummy destination P' for the continuous warping is defined as the closest point to the physical target P that lies on the direct connection of V and P but still is inside the unnoticeability area. As can be seen from Fig. 3, potential optimal P' locations are:

1. P – the physical target itself, if within the unnoticeability area
2. $P'_{\beta_{max},\{right, left\}}$ – points where β_{max} is exceeded
3. $P'_{g_{max},\{1,2\}}$ – points where g_{max} is exceeded
4. $P'_{g_{min},\{1,2\}}$ – points where g_{min} is exceeded

To determine P' , the algorithm computes all of these points using 3D line intersection methods. The computation of $P'_{g_{max},\{1,2\}}$, for example, is implemented by computing a 3D line-sphere intersection between the line r (covering the ray from V towards P) with:

$$r : V + t \cdot (P - V) \quad t \in \mathbb{R} \quad (5)$$

and a sphere at the origin O with radius $g_{max} \cdot |(V - O)|$, the surface of which geometrically represents the g_{max} threshold. The intersection of r with this sphere thus represents the position along r at which the g_{max} threshold is exceeded. In the same way, the points along r at which the g_{min} threshold is exceeded can also be computed by intersecting r against a sphere at O with radius $g_{min} \cdot |(V - O)|$. As the ray origin V does not lie inside this sphere, here, either 2, 1, or no intersections exist. Finally, the geometric representation of the angular threshold β_{max} is two lines, which can be defined by rotating the vector from O to V to the $\{right, left\}$ by angle β_{max} . To find $P'_{\beta_{max},\{right, left\}}$, the intersections of r with these lines are also computed. For computational robustness, we represented the β_{max} lines as two 3D planes and computed line-plane intersections.

Each of the computed intersections is represented by a value $t \in \mathbb{R}$ (see Equation 5) denoting the relative position of the intersection

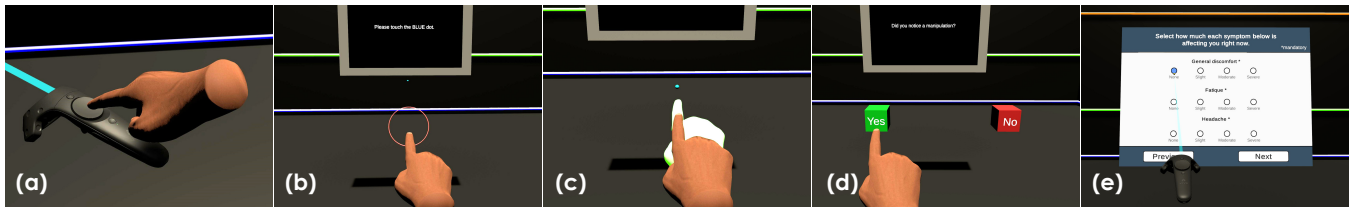


Figure 4: VR view of the experiment: (a) fingertip calibration in between experimental blocks; (b) circular area the participant's fingertip needs to pass through to start the next trial; (c) the virtual hand offset *towards* the user approaching the target location V (the redirected real hand location is highlighted in white here for illustration only); (d) the yes/no question; (e) the SSQ questionnaire.

along the line ($t = 0$ representing V ; $t = 1$ representing P). To determine P' as the location that is closest to the target P but still within *all* thresholds, the BSHR algorithm sorts all corresponding $t \geq 0$ in ascending order, resulting in a list where t_0 is the minimum, and t_6 the maximum value:

$$\text{sort}(\{t_P, t_{\beta_{\max, \text{right}}}, \dots, t_{g_{\min}, 2}\}) = [t_0, t_1, \dots, t_6] \quad (6)$$

Accounting for a special case where the g_{\min} sphere is intersected twice, i.e. the threshold is first exceeded and then met again before any other threshold is exceeded, the algorithm finally returns:

$$P' = \begin{cases} V + t_2 \cdot (P - V), & \text{if } t_0 \text{ and } t_1 \text{ belong to } g_{\min} \\ V + t_0 \cdot (P - V), & \text{else} \end{cases} \quad (7)$$

The following section summarizes our evaluation of BSHR.

4 EVALUATION

We conducted a psychophysical user experiment to study the detectability of the BSHR approach. Our goal was to validate the feasibility of leveraging blink suppression for unnoticeable hand redirection in VR. To this end, we estimate the conservative detection thresholds (CDTs) of 4 hand redirection techniques:

1. $BSHR_{+0\%}$: Pure BSHR (Mode 1); no continuous redirection.
2. $BSHR_{+50\%}$: Combined (Mode 2); additional continuous redirection up to 50% of detection thresholds [58] (cf. **H2a**, **H2b**).
3. $BSHR_{+100\%}$: Combined (Mode 2); additional continuous redirection up to 100% of detection thresholds [58] (cf. **H2a**, **H2b**).
4. *Cheng*: Cheng et al.'s [9] approach; unlimited continuous redirection only.

While the $BSHR_{+0\%}$ condition offsets the hand only instantaneously during blink suppression, $BSHR_{+50\%}$ and $BSHR_{+100\%}$ additionally redirect the hand when the eyes are open by applying continuous warps up to 50% and 100% of the detection thresholds in assumption 3, respectively. *Cheng* does not utilize any instantaneous shifts, but only applies unlimited continuous redirection [9].

In line with previous research [4, 58], we restrict our investigation to the 3 central axes (horizontal, vertical, and gain). To prevent effects of fatigue and to maintain an acceptable experimentation time, we estimate the threshold of each participant and each of the 4 techniques for 3 representative directions:

1. *right*: the virtual hand is offset towards the right (+X).
2. *down*: the virtual hand is offset downwards (-Y).
3. *towards*: the virtual hand is offset towards the user (-Z).

4.1 Hypotheses

Our study is designed to evaluate 4 central hypotheses. First, we expected unnoticeable, pure blink-suppressed hand redirection (*Mode 1* – $BSHR_{+0\%}$) to be feasible in practice, i.e. achieving an unnoticeability range significantly greater than 0cm (**H1**). As no detection thresholds for the original approach by Cheng et al. [9] have been determined in previous research, secondly, we expected *Cheng* to go unnoticed within the thresholds found by related work investigating a similar hand warping technique [58] (**H2**). Regarding the

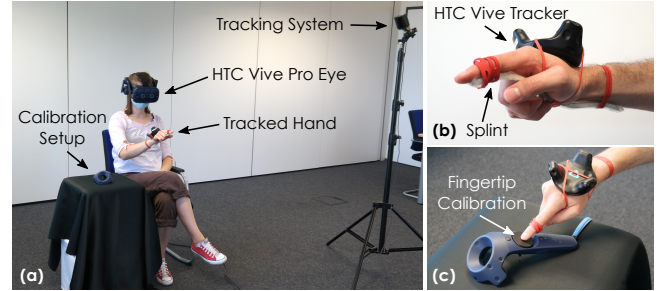


Figure 5: Experimental setup: (a) shows the real environment with the tracking system and calibration pedestal; (b) depicts the hand tracking rig; (c) shows the calibration of the fingertip \leftrightarrow tracker offset [58].

combined redirection approach (*Mode 2*), we expected the range of unnoticeable BSHR to increase with additional continuous warping in $BSHR_{+50\%}$ and $BSHR_{+100\%}$ (**H3**). Finally, we hypothesized the CDTs of $BSHR_{+100\%}$ to exceed the CDTs of *Cheng* (**H4**). Formally:

1. **H1**: $\text{CDT}_{\text{all dir.}}(BSHR_{+0\%}) > 0$
2. **H2a**: $\text{CDT}_{\{\text{right, down}\}}(\text{Cheng}) \geq \beta_{\max} = 4.5^\circ$ [58] $\Rightarrow 3.15\text{cm}$
H2b: $\text{CDT}_{\{\text{towards}\}}(\text{Cheng}) \geq g_{\max} = 1.14$ [58] $\Rightarrow 5.5\text{cm}$
3. **H3a**: $\text{CDT}_{\text{all dir.}}(BSHR_{+0\%}) < \text{CDT}_{\text{all dir.}}(BSHR_{+50\%})$
H3b: $\text{CDT}_{\text{all dir.}}(BSHR_{+50\%}) < \text{CDT}_{\text{all dir.}}(BSHR_{+100\%})$
4. **H4**: $\text{CDT}_{\text{all dir.}}(\text{Cheng}) < \text{CDT}_{\text{all dir.}}(BSHR_{+100\%})$

4.2 Participants

17 volunteers were recruited from the local campus. $N = 15$ participants (7f; 8m) completed the experiment. Two participants were excluded as the staircase procedure for one of them did not converge, while the experiment took too long for the other excluded participant. Participants were on average 25.5 years old ($SD = 3.5$ years; min. 20 years; max. 33 years). Assessed on a scale from 1 = never to 7 = regularly, our participants covered a wide range of previous experience levels with 3D video games ($M = 3.8$ ($SD = 2.65$); min. 1; max. 7), VR ($M = 2.6$ ($SD = 1.73$); min. 1; max. 7) and manual crafting ($M = 4.4$ ($SD = 1.41$); min. 2; max. 7).

4.3 Apparatus

Our study took place in a lab at our institution. The setup can be seen in Fig. 5. We used a HTC Vive Pro Eye HMD, a HTC Vive Pro Controller, and a HTC Vive Tracker (v2018) tracked with SteamVR base stations 2.0. A notebook with an NVIDIA GTX 1070 graphics card was used to run the study software implemented with *Unity 2019.3.0f6*, the *VRQuestionnaireToolkit*² [16], the *Unity Ex-*

²<https://github.com/MartinFk/VRQuestionnaireToolkit>

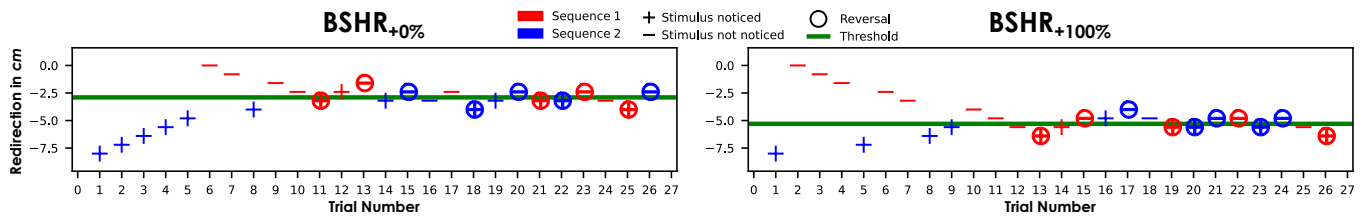


Figure 6: Staircase results of participant #1 for virtual hand offsets towards the *right*. An increase in detection threshold can be observed when continuous warping is added in $BSHR_{+100\%}$ (right) compared to the pure blink-suppressed instantaneous warping in $BSHR_{+0\%}$ (left).

periment Framework³ [7], and the *SRanipal SDK*⁴ for eye tracking. To track the dominant hand of participants, we applied a solution proposed in related work [58], utilizing a tracker attached with a rubber band to the back of the hand. To maintain calibration and a static hand pose, participants wore a finger splint as shown in Fig. 5 (b), which fixed the offset of the tracker on the back of the hand to the fingertip. This offset was (re-)calibrated before each experimental block. For this, participants repeatedly touched the touch-sensitive trackpad on the controller, as shown in Fig. 5 (c).

4.4 Procedure

Upon providing informed consent and basic demographic data, participants put on the VR equipment and sat down on a chair inside the tracking volume (Fig. 5 (a)). For hand calibration, the Vive controller was placed on a small pedestal next to the participant and the offset from the fingertip to the Vive tracker was calibrated as shown in Fig. 4 (a) and Fig. 5 (c). Lastly, the IVE was calibrated.

Participants then started to practice the experimental trials in 2 test blocks ($BSHR_{+0\%}$ and *Cheng*; random directions), before the actual experiment and data recording began. To complete the experiment, each participant had to complete 12 blocks (a threshold estimation procedure for each of the 4 techniques in each of the 3 directions). To complete a block, a simple trial was repeated several times. In a trial, users were asked to reach towards a small virtual sphere initially rendered 125cm in front of them. When passing with their finger through a circular zone with radius 5cm centered 30cm below and 25cm straight in front of their head (highlighted in Fig. 4 (b)), hand redirection and blink detection was activated and the virtual sphere relocated to the virtual target position V of the trial. V was located 40cm straight in front of their fingertip location when passing through the circular zone as in the experiment of Zenner and Krüger [58]. While reaching for the target (Fig. 4 (c)), the corresponding redirection algorithm was applied, with the real target position P being offset from V along the axis corresponding to the block. The amount of offset between real and virtual target (between P and V) varied across trials following an interleaved staircase procedure, as described in the following section. To ensure conservativeness, participants were instructed to pay close attention to detecting any signs of redirection, and were told that both continuous and sudden hand offsets could occur at any time. Moreover, participants were asked to blink frequently throughout the experiment (across all techniques) and informed that only trials in which they blinked at least once during the reach could be used for analysis. However, participants were intentionally not told about the fact that if a trial was determined to be invalid, the trial was completed as usual, with the offset being repeated immediately in the following trial. To ensure that each trial used in the analysis met assumptions 1 and 2, a trial was considered invalid if the participant did not blink at all during the reach, or blinked but assumption 2 was not met. These

requirements applied to all conditions to ensure comparability. To end a trial when the virtual finger reached V , participants responded to the yes/no question “Did you notice a manipulation?” (Fig. 4 (d)). After answering, the virtual target sphere relocated to its initial position and participants continued with the next trial in the block until the respective staircase procedure, and with it the block, terminated. In between blocks, participants were instructed to rest for at least 30s and to re-calibrate. After completion of all 12 blocks, the SUS presence questionnaire [44], Simulator Sickness Questionnaire [26], and a concluding questionnaire were filled out in VR (Fig. 4 (e)).

4.5 Design

Our study has a within-subject design with two independent variables: redirection algorithm (4 techniques) and direction (3 directions). This results in 12 blocks per participant. We used a 12x12 Williams design Latin square [55] to counterbalance blocks across participants. For each block, we employed a psychophysical detection threshold estimation method [27], specifically a 1 up/1 down method [28], to approximate for each algorithm and direction the participant’s conservative detection threshold (CDT). The CDT, being the dependent variable in our study, represents the amount of redirection in *cm* that goes unnoticed when applying the respective algorithm in the respective direction. We used an interleaved staircase implementation with an ascending (starting at the min. redirection of 0cm) and a descending (starting at the max. redirection of 8cm; determined during piloting) sequence, using a constant step size of 0.8cm. If participants noticed the redirection in a trial (answering *yes*), the amount of redirection in the following trial of that sequence was decreased by the step size; otherwise (answering *no*) it was increased by the step size. A sequence terminated after 5 reversals, with the average of the last 4 reversals being taken as the sequence threshold estimate. The average of the ascending and descending sequence thresholds yielded the CDT.

4.6 Results

The SUS count ($M = 1.87$ ($SD = 1.60$); min. 0; max. 5) and SUS mean ($M = 4.61$ ($SD = 0.97$); min. 2.33; max. 6.33) scores verified our IVE to be generally immersive, while a relatively low SSQ total score ($M = 38.15$, $SD = 32.33$) did not indicate any cybersickness issues. In total, 6739 trials ($M = 449.3$, $SD = 121.6$ per participant) were completed, out of which 4581 trials ($M = 305.4$, $SD = 19.6$ p. p.) were valid and contributed to our analysis. The valid blinks of our participants lasted 115.9ms on average ($SD = 34.5ms$). When blinking validly, participants closed their eyes when their hand had traveled 46.19% on average ($SD = 13.83\%$) along the way towards the target, and opened them again at 52.61% on average ($SD = 13.74\%$). To study our hypotheses, we analyzed the CDTs obtained for the 12 conditions, applying a significance level of $\alpha = .05$.

4.6.1 H1: Detectability of $BSHR_{+0\%}$

To investigate **H1**, we compared the obtained detection thresholds of $BSHR_{+0\%}$ for each direction against 0cm. After normality of the respective data was confirmed by a Shapiro-Wilk test, we performed 3

³<https://github.com/immersivecognition/unity-experiment-framework>

⁴<https://developer.vive.com/resources/vive-sense/sdk/vive-eye-tracking-sdk-sranipal/>

Table 1: The detection thresholds obtained for the 4 tested techniques when applied in each of the 3 directions. p' columns indicate the corrected p -values; significant differences are highlighted in green. The top row indicates to which hypotheses the respective comparisons belong. An increase of the unnoticeability range can be observed when increasing the continuous warping in the BSHR approach.

Direction	H1			H3			H4			H2	
	Baseline	p'	$BSHR_{+0\%}$	p'	$BSHR_{+50\%}$	p'	$BSHR_{+100\%}$	p'	Cheng	p'	Cheng _{exp}
<i>right</i>	0cm	< .001	M = 2.65cm SD = 1.26cm	< .038	M = 3.56cm SD = 1.27cm	< .038	M = 4.34cm SD = 1.47cm	< .027	M = 5.81cm SD = 1.98cm	< .006	3.148cm
<i>down</i>	0cm	< .001	M = 3.83cm SD = 1.11cm	< .045	M = 4.94cm SD = 1.47cm	= .372	M = 5.39cm SD = 1.23cm	= .64	M = 5.63cm SD = 2.13cm	< .006	3.148cm
<i>towards</i>	0cm	< .001	M = 3.27cm SD = 1.66cm	= .076	M = 4.26cm SD = 1.73cm	= .076	M = 4.36cm SD = 1.23cm	= .076	M = 4.63cm SD = 1.88cm	= .519	5.5cm

one-sample t-tests with Bonferroni correction (corrected p values denoted as p'). The range of unnoticeable blink-suppressed hand redirection using $BSHR_{+0\%}$ with virtual hand offsets in direction *right* ($M = 2.65cm$, $SD = 1.26cm$), *down* ($M = 3.83cm$, $SD = 1.11cm$), and *towards* the user ($M = 3.27cm$, $SD = 1.66cm$) were all found to be statistically significant greater than 0cm (all $p' < .001$).

4.6.2 H2: Detectability of Cheng

To confirm **H2**, i.e. our assumption that continuous redirection as in the *Cheng* algorithm goes unnoticed within the unnoticeability ranges found for a similar technique in related work [9, 58], we compared the thresholds obtained for *Cheng* against these expected values. Since a Shapiro-Wilk test indicated a violation of the normality assumption ($p < .05$), we applied 3 one-sample Wilcoxon tests with Bonferroni correction. The results indicate the amount of unnoticeable redirection with the *Cheng* method to significantly exceed the expected min. threshold of 3.15cm (i.e. 4.5° in a distance of 40cm [58]) for *right* ($M = 5.81cm$, $SD = 1.98cm$) and *down* ($M = 5.63cm$, $SD = 2.13cm$) (both $p' \leq .006$). The thresholds *towards* the user ($M = 4.63cm$, $SD = 1.88cm$) were not found to differ significantly from the expected threshold of 5.5cm (i.e. the real hand grasping 13.75% further than the virtual hand [58]) ($p' = .519$).

4.6.3 H3 & H4: Detectability of Combined Redirection

To analyze **H3** and **H4**, we compared the thresholds of the 4 redirection techniques for each direction. Since normality could not be assumed in all cases according to Shapiro-Wilk tests, we performed a non-parametric Friedman test for each direction. To find pairwise differences, we applied post-hoc Wilcoxon signed-rank tests with Bonferroni-Holm correction. Fig. 7 shows the obtained thresholds and indicates significant pairwise differences. Fig. 6 shows a representative staircase plot and Table 1 summarizes the results.

For direction *right* ($\chi^2(3) = 28.034$, $p < .001$) and *down* ($\chi^2(3) = 14.331$, $p \leq .002$), the Friedman tests indicated thresholds differed significantly across the techniques. Post-hoc results for *right* showed each individual technique to yield an unnoticeability range that is significantly different from any other technique's range (all $p' \leq .038$). For *down*, the pairwise test only showed the thresholds of $BSHR_{+0\%}$ to differ significantly from those of $BSHR_{+50\%}$ and $BSHR_{+100\%}$ (both $p' \leq .045$). For *towards*, the Friedman test did not indicate thresholds to differ significantly ($\chi^2(3) = 6.872$, $p = .076$).

Most importantly regarding **H3**, the hypothesized rise in detection thresholds from $BSHR_{+0\%}$ to $BSHR_{+50\%}$ was statistically confirmed for *right* (from $M = 2.65cm$ ($SD = 1.26cm$) to $M = 3.56cm$ ($SD = 1.27cm$); $Z = -2.355$, $p' \leq .038$, $r = .43$) and *down* (from $M = 3.83cm$ ($SD = 1.11cm$) to $M = 4.94cm$ ($SD = 1.47cm$); $Z = -2.613$, $p' \leq .045$, $r = .48$). The hypothesized increase from $BSHR_{+50\%}$ to $BSHR_{+100\%}$ was statistically significant only for *right* (from $M = 3.56cm$ ($SD = 1.27cm$) to $M = 4.34cm$ ($SD = 1.47cm$); $Z = -2.133$, $p' \leq .038$, $r = .39$).

Analyzing **H4**, the *right* threshold of $BSHR_{+100\%}$ ($M = 4.34cm$, $SD = 1.47cm$) was, in contrast to our expectations, significantly smaller than that of *Cheng* ($M = 5.81cm$, $SD = 1.98cm$)

($Z = -2.616$, $p' \leq .027$, $r = .48$). For *down* and *towards*, differences between $BSHR_{+100\%}$ and *Cheng* were non-significant.

5 DISCUSSION

Our results validate the feasibility of blink-suppressed hand redirection and point to the value of combining it with continuous warping.

5.1 The Detectability of $BSHR_{+0\%}$ and Cheng

Studying $BSHR_{+0\%}$, i.e. the application of only instantaneous hand shifts during blinks, revealed detection thresholds significantly greater than 0cm for each tested direction (column $BSHR_{+0\%}$ in Table 1). This result confirms **H1** and proves the practical feasibility of pure BSHR. The unnoticeability ranges found for $BSHR_{+0\%}$ correspond to 3.79° and 5.47° for *right* and *down* respectively, and to a gain factor of 1.08 for *towards*, and are thus of the same order of magnitude as the CDTs found for continuous hand warping in previous work [58]. Our results demonstrate for the first time that these ranges of unnoticeable hand redirection can also be achieved by only leveraging periods of blink suppression, instead of applying manipulations while users observe the scene with opened eyes.

Observations of the opposite extreme, i.e. pure incremental warping as in the *Cheng* condition, also revealed corresponding thresholds (column *Cheng* in Table 1). We found the range of unnoticeable *Cheng* redirection along the horizontal and vertical axis to be significantly greater than the minimum expected range [58]. The unnoticeability range along the depth axis was only non-significantly below the expected range of 5.5cm. Our results thus also support **H2** and validate assumption 3: our expectation that within the thresholds found by previous work, the incremental warping applied in our implementation also goes unnoticed. Consequently, the derived CDTs back our concept of combining incremental warps below the thresholds specified in Sect. 3.2 with instantaneous shifts during blink suppression, and support the results of related literature [58].

5.2 The Detectability of Combined Redirection

With **H3** we investigated if combining instantaneous hand shifts during blinks and continuous warping with opened eyes has any effect on detection thresholds. As can be seen from Table 1, the average range of unnoticeable redirection *increased* with increasing amounts of continuous warping added to the BSHR approach for every tested direction. Our statistical evidence, however, only partially supports **H3** as this rise in thresholds was found to be statistically significant only for *right* and partially for *down*. From our observations, users seemed to detect manipulations along the depth axis more easily. This seems backed by Benda et al. [4] and might be related to how sensory integration is affected by direction [52]. We speculate that this special role of depth might have contributed to the fact that an increase of thresholds did not become statistically striking for *towards*. Nonetheless, our data indicates a general tendency of thresholds to increase when combining both approaches, compared to pure BSHR.

The central idea of the proposed approach, i.e. allowing for as much continuous warping when the user looks at the scene as goes unnoticed, was implemented based on results of previous work [58], but can now be refined using the results of our study. Having derived

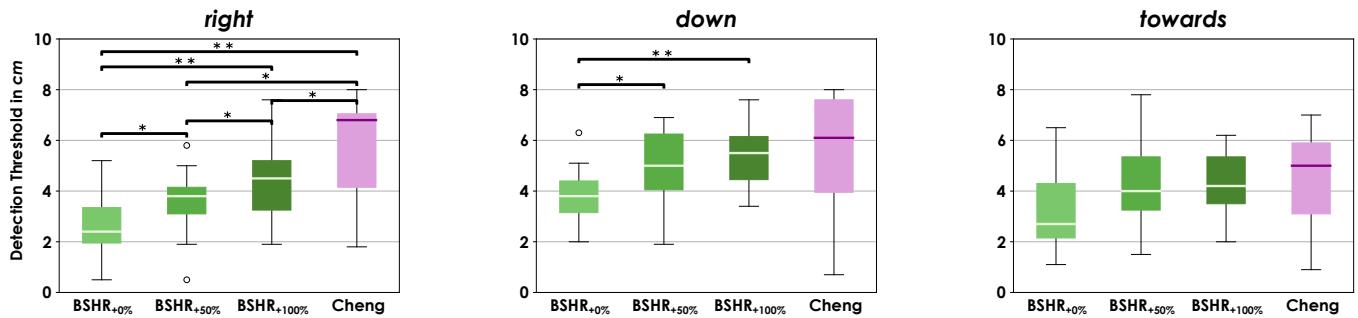


Figure 7: Box plots showing the detection thresholds, i.e. the range of unnoticeable redirection, of the 4 compared techniques for each of the 3 tested directions. Brackets indicate statistically significant differences ($p' < .05$ (*); $p' < .01$ (**)).

CDT estimates for the algorithm by Cheng et al. [9], the BSHR parameters can now be fine-tuned. Specifically, we recommend replacing the unnoticeability range defined in assumption 3 in Sect. 3.2 with the now-known thresholds of Cheng summarized in Table 1. In line with this, we speculate that thresholds can be further increased, maybe even up to a point where the combined technique allows for more redirection to go unnoticed than the continuous approach. This might occur if the entire unnoticeability range of the continuous approach is leveraged while users look at the scene, and an additional unnoticeable offset is introduced when the vision of users is suppressed. While we hypothesized this effect to occur already in our study, **H4** was not supported by the results as thresholds of $BSHR_{+100\%}$ did not exceed those of Cheng along any axis in our experiment. We suspect this to be a consequence of the non-optimal selection of the parameters β_{max} , g_{min} , and g_{max} , which were not directly based on the applied Cheng technique. For example, the threshold of Cheng for offsets towards the user was lower than the configured range in $BSHR_{+100\%}$ of 5.5cm. Consequently, participants might have noticed the incremental warping in $BSHR_{+100\%}$ even before any offset was added during a blink. In the case of right and down, on the other hand, more continuous warping would have been possible within the unnoticeability ranges of Cheng than configured based on assumption 3. Hence, blink warps were applied “too early”, i.e. already for redirections smaller than necessary, and participants might have noticed these offsets added during blinks even for redirections below the Cheng thresholds. We are optimistic, however, that with more participant-specific parameters, combined redirection might achieve larger unnoticeability ranges than both individual approaches. A per-user calibration might help to determine the most optimal β_{max} , g_{min} , and g_{max} for each individual.

5.3 Limitations & Future Work

The BSHR algorithm proposed in this paper is designed to allow for a first controlled investigation of the detection thresholds of blink-suppressed hand redirection. To reliably redirect the user’s real hand to reach P , however, assumptions 1 and 2 (Sect. 3.2) have to be fulfilled. These assumptions are to ensure consistency and comparability of our results, but limit the usability of BSHR as proposed in this paper. We thus aim to evolve the BSHR approach in future work, e.g. by integrating a fail-safe mechanism. Such a mechanism could ensure that the user will reach the physical destination in all circumstances by sacrificing unnoticeability and boosting the continuous warping if the user does not blink. If the algorithm detects, for example, that no blink has occurred while the virtual hand progressed $X\%$ along the way towards V , a fallback warping towards P could be applied, exceeding detection thresholds. Figuring out optimal values for X and suitable fallback warping strategies are interesting avenues for future work. We would also like to study alternative mechanisms that let the system trigger blinks as needed, and investigate their effects on detection thresholds. Blinks could

potentially be triggered by simulating natural reasons for blinking in VR, such as a blurred view, sudden changes in brightness, or the like [11]. To provide optimal grounds for a technique like BSHR, the IVE itself might also be designed to trigger blinks when the hands must be redirected, e.g. by guiding the user’s attention in a way that promotes blinking, similar to how the user’s attention is directed in systems employing change blindness haptic remapping [32]. Moreover, similar to how distractors are employed for RDW [10], distractors that trigger blinks could be developed to grant the system some control over the user’s blink frequency. Beyond leveraging blink suppression, we plan to further evolve our approach to also make use of saccadic suppression. This would open many more opportunities for injecting hand offsets, each of which would be much shorter, however. Finally, we would like to study how a per-user calibration could automatically select optimal parameters with minimal setup effort.

6 CONCLUSION

We expand the list of HR techniques by presenting the first approach that takes advantage of blink-induced change blindness. Motivated by recent advances that leveraged blink suppression to implement RDW [30, 35], we designed the Blink-Suppressed Hand Redirection (BSHR) algorithm with the goal to study the approach’s feasibility and noticeability. Our technique applies instantaneous hand offsets when the user’s vision is temporarily suppressed during a blink. By configuring an unnoticeability range around the virtual target, the algorithm can additionally combine continuous hand redirection with blink-suppressed shifts. In this combined mode, BSHR introduces continuous offsets below detection thresholds while the user’s eyes are opened, and additionally alters hand offsets when the user’s eyes are closed. By studying our technique in a psychophysical experiment, we derived conservative detection thresholds for pure blink-suppressed hand redirection ($BSHR_{+0\%}$), for combined continuous warping and blink-suppressed redirection ($BSHR_{+50\%}$ and $BSHR_{+100\%}$), as well as for the technique by Cheng et al. [9] (Cheng) that does not leverage blinks. Our results verify the feasibility of blink-suppressed body warping as we found ranges of unnoticeable redirection in the same order of magnitude as found for conventional techniques. Moreover, we could show that for redirection along the horizontal and vertical axis, more redirection can go unnoticed when combining continuous warping and instantaneous blink-suppressed shifts compared to pure blink-suppressed redirection. These promising first results encourage continuing the exploration of techniques that take advantage of change blindness and the phenomenon of visual suppression to realize hand redirection in VR.

ACKNOWLEDGMENTS

The authors wish to thank all participants of the study. This research was funded by the Deutsche Forschungsgemeinschaft (DFG, German Research Foundation) – project number 425868555; 450247716.

REFERENCES

- [1] P. Abtahi and S. Follmer. Visuo-haptic illusions for improving the perceived performance of shape displays. In *Proc. CHI*, pp. 150:1–150:13. ACM, New York, NY, USA, 2018. doi: 10.1145/3173574.3173724
- [2] P. Abtahi, B. Landry, J. J. Yang, M. Pavone, S. Follmer, and J. A. Landay. Beyond the force: Using quadcopters to appropriate objects and the environment for haptics in virtual reality. In *Proc. CHI*, pp. 359:1–359:13. ACM, New York, NY, USA, 2019. doi: 10.1145/3290605.3300589
- [3] M. Azmandian, M. Hancock, H. Benko, E. Ofek, and A. D. Wilson. Haptic Retargeting: Dynamic repurposing of passive haptics for enhanced virtual reality experiences. In *Proc. CHI*, pp. 1968–1979. ACM, New York, NY, USA, 2016. doi: 10.1145/2858036.2858226
- [4] B. Benda, S. Esmaili, and E. D. Ragan. Determining detection thresholds for fixed positional offsets for virtual hand remapping in virtual reality. In *Proc. ISMAR*, pp. 269–278. IEEE, Nov 2020. doi: 10.1109/ISMAR50242.2020.00050
- [5] B. Bolte and M. Lappe. Subliminal reorientation and repositioning in immersive virtual environments using saccadic suppression. *IEEE Transactions on Visualization and Computer Graphics*, 21(4):545–552, 2015. doi: 10.1109/TVCG.2015.2391851
- [6] D. Bristow, J.-D. Haynes, R. Sylvester, C. D. Frith, and G. Rees. Blinking suppresses the neural response to unchanging retinal stimulation. *Current Biology*, 15(14):1296–1300, Jul 2005. doi: 10.1016/j.cub.2005.06.025
- [7] J. Brookes, M. Warburton, M. Alghadier, M. Mon-Williams, and F. Mushtaq. Studying human behavior with virtual reality: The Unity Experiment Framework. *Behavior Research Methods*, 52:455–463, 2020. doi: 10.3758/s13428-019-01242-0
- [8] E. Burns, S. Razzaque, A. T. Panter, M. C. Whitton, M. R. McCallus, and J. Frederick P. Brooks. The hand is more easily fooled than the eye: Users are more sensitive to visual interpenetration than to visual-proprioceptive discrepancy. *Presence: Teleoperators and Virtual Environments*, 15(1):1–15, Feb. 2006. doi: 10.1162/pres.2006.15.1.1
- [9] L.-P. Cheng, E. Ofek, C. Holz, H. Benko, and A. D. Wilson. Sparse Haptic Proxy: Touch feedback in virtual environments using a general passive prop. In *Proc. CHI*, pp. 3718–3728. ACM, New York, NY, USA, 2017. doi: 10.1145/3025453.3025753
- [10] R. Cools and A. L. Simeone. Investigating the effect of distractor interactivity for redirected walking in virtual reality. In *Proc. SUI*, SUI, pp. 1–5. ACM, New York, NY, USA, 2019. doi: 10.1145/3357251.3357580
- [11] T. Cmovrsanin, Y. Wang, and K.-L. Ma. Stimulating a blink: Reduction of eye fatigue with visual stimulus. In *Proc. CHI*, p. 2055–2064. ACM, New York, NY, USA, 2014. doi: 10.1145/2556288.2557129
- [12] M. S. Dennison, A. Z. Wisti, and M. D'Zmura. Use of physiological signals to predict cybersickness. *Displays*, 44:42–52, 2016. Contains Special Issue Articles – Proceedings of the 4th Symposium on Liquid Crystal Photonics (SLCP 2015). doi: 10.1016/j.displa.2016.07.002
- [13] L. Dominjon, A. Lécuyer, J. M. Burkhardt, P. Richard, and S. Richir. Influence of control/display ratio on the perception of mass of manipulated objects in virtual environments. In *Proc. VR*, pp. 19–25. IEEE Computer Society, Mar 2005. doi: 10.1109/VR.2005.1492749
- [14] M. J. Doughty. Further assessment of gender- and blink pattern-related differences in the spontaneous eyeblink activity in primary gaze in young adult humans. *Optometry and Vision Science*, 79(7), 2002. doi: 10.1097/00006324-200207000-00013
- [15] S. Esmaili, B. Benda, and E. D. Ragan. Detection of scaled hand interactions in virtual reality: The effects of motion direction and task complexity. In *Proc. VR*, pp. 453–462. IEEE, 2020. doi: 10.1109/VR46266.2020.00066
- [16] M. Feick, N. Kleer, A. Tang, and A. Krüger. The Virtual Reality Questionnaire Toolkit. In *Adjunct Proc. UIST*. ACM, 2020. doi: 10.1145/3379350.3416188
- [17] J. Fitzakerley. Eyelid Movements. Online. <https://www.d.umn.edu/~jfitzake/Lectures/DMED/Vision/Optics/Blinking.html> [Last accessed on Sep. 30, 2020], 2015.
- [18] J. J. Gibson. Adaptation, after-effect and contrast in the perception of curved lines. *Journal of Experimental Psychology*, 16(1):1–31, 1933. doi: 10.1037/h0074626
- [19] E. J. Gonzalez, P. Abtahi, and S. Follmer. Reach+: Extending the reachability of encountered-type haptics devices through dynamic redirection in VR. In *Proc. UIST*, pp. 236–248. ACM, New York, NY, USA, 2020. doi: 10.1145/3379337.3415870
- [20] E. J. Gonzalez and S. Follmer. Investigating the detection of bimanual haptic retargeting in virtual reality. In *Proc. VRST*. ACM, New York, NY, USA, 2019. doi: 10.1145/3359996.3364248
- [21] D. T. Han, M. Suhail, and E. D. Ragan. Evaluating remapped physical reach for hand interactions with passive haptics in virtual reality. *IEEE Transactions on Visualization and Computer Graphics*, 24(4):1467–1476, April 2018. doi: 10.1109/TVCG.2018.2794659
- [22] K. Hinckley, R. Pausch, J. C. Goble, and N. F. Kassell. Passive real-world interface props for neurosurgical visualization. In *Proc. CHI*, pp. 452–458. ACM, New York, NY, USA, 1994. doi: 10.1145/191666.191821
- [23] B. E. Insko. *Passive Haptics Significantly Enhances Virtual Environments*. PhD thesis, University of North Carolina at Chapel Hill, USA, 2001.
- [24] D. A. G. Jauregui, F. Argelaguet, A. H. Olivier, M. Marchal, F. Multon, and A. Lécuyer. Toward pseudo-haptic avatars: Modifying the visual animation of self-avatar can simulate the perception of weight lifting. *IEEE Transactions on Visualization and Computer Graphics*, 20(4):654–661, Apr 2014. doi: 10.1109/TVCG.2014.45
- [25] J. Jerald. *The VR Book: Human-Centered Design for Virtual Reality*. Association for Computing Machinery and Morgan & Claypool, New York, NY, USA, 2016. doi: 10.1145/2792790
- [26] R. S. Kennedy, N. E. Lane, K. S. Berbaum, and M. G. Lilienthal. Simulator Sickness Questionnaire: An enhanced method for quantifying simulator sickness. *The International Journal of Aviation Psychology*, 3(3):203–220, 1993. doi: 10.1207/s15327108ijap0303_3
- [27] F. A. Kingdom and N. Prins. Chapter 2 - Classifying Psychophysical Experiments. In *Psychophysics - A Practical Introduction (Second Edition)*, pp. 11–35. Academic Press, San Diego, second ed., 2016. doi: 10.1016/B978-0-12-407156-8.00002-5
- [28] F. A. Kingdom and N. Prins. Chapter 5 - Adaptive Methods. In *Psychophysics - A Practical Introduction (Second Edition)*, pp. 119–148. Academic Press, San Diego, second ed., 2016. doi: 10.1016/B978-0-12-407156-8.00005-0
- [29] L. Kohli. *Redirected Touching*. PhD thesis, University of North Carolina at Chapel Hill, USA, 2013.
- [30] E. Langbehn, F. Steinicke, M. Lappe, G. F. Welch, and G. Bruder. In the blink of an eye: Leveraging blink-induced suppression for imperceptible position and orientation redirection in virtual reality. *ACM Trans. Graph.*, 37(4), July 2018. doi: 10.1145/3197517.3201335
- [31] R. J. Leigh and D. S. Zee. *The Neurology of Eye Movements*. Oxford University Press, Oxford, UK, 5th ed., 06 2015. doi: 10.1093/med/9780199969289.001.0001
- [32] A. L. Lohse, C. K. Kjær, E. Hamulic, I. G. A. Lima, T. H. Jensen, L. E. Bruni, and N. C. Nilsson. Leveraging change blindness for haptic remapping in virtual environments. In *Proc. WEVR*, pp. 1–5, 2019. doi: 10.1109/WEVR.2019.8809587
- [33] S. Marwecki, A. D. Wilson, E. Ofek, M. Gonzalez Franco, and C. Holz. Mise-unseen: Using eye tracking to hide virtual reality scene changes in plain sight. In *Proc. UIST*, pp. 777–789. ACM, New York, NY, USA, 2019. doi: 10.1145/3332165.3347919
- [34] R. A. Montano Murillo, S. Subramanian, and D. Martinez Plasencia. Erg-O: Ergonomic optimization of immersive virtual environments. In *Proc. UIST*, pp. 759–771. ACM, New York, NY, USA, 2017. doi: 10.1145/3126594.3126605
- [35] A. Nguyen and A. Kunz. Discrete scene rotation during blinks and its effect on redirected walking algorithms. In *Proc. VRST*. ACM, New York, NY, USA, 2018. doi: 10.1145/3281505.3281515
- [36] N. C. Nilsson, T. Peck, G. Bruder, E. Hodgson, S. Serafin, M. Whitton, F. Steinicke, and E. S. Rosenberg. 15 years of research on redirected walking in immersive virtual environments. *IEEE Computer Graphics and Applications*, 38(2):44–56, 2018. doi: 10.1109/MCG.2018.111125628
- [37] N. Ogawa, T. Narumi, and M. Hirose. Effect of avatar appearance on detection thresholds for remapped hand movements. *IEEE Transactions on Visualization and Computer Graphics*, pp. 1–1, 2020. doi: 10.1109/TVCG.2020.2964758

- [38] S. Patel, R. Henderson, L. Bradley, B. Galloway, and L. Hunter. Effect of visual display unit use on blink rate and tear stability. *Optometry and Vision Science*, 68(11), 1991. doi: 10.1097/00006324-199111000-00010
- [39] I. Poupyrev, M. Billinghurst, S. Weghorst, and T. Ichikawa. The Go-Go interaction technique: Non-linear mapping for direct manipulation in VR. In *Proc. UIST*, pp. 79–80. ACM, New York, NY, USA, 1996. doi: 10.1145/237091.237102
- [40] S. Razzaque. *Redirected Walking*. PhD thesis, University of North Carolina at Chapel Hill, USA, 2005.
- [41] M. Rietzler, F. Geiselhart, J. Gugenheimer, and E. Rukzio. Breaking the tracking: Enabling weight perception using perceivable tracking offsets. In *Proc. CHI*, pp. 1—12. ACM, New York, NY, USA, 2018. doi: 10.1145/3173574.3173702
- [42] M. Samad, E. Gatti, A. Hermes, H. Benko, and C. Parise. Pseudo-haptic weight: Changing the perceived weight of virtual objects by manipulating control-display ratio. In *Proc. CHI*, pp. 1—13. ACM, New York, NY, USA, 2019. doi: 10.1145/3290605.3300550
- [43] D. J. Simons and D. T. Levin. Change blindness. *Trends in Cognitive Sciences*, 1(7):261–267, 1997. doi: 10.1016/S1364-6613(97)01080-2
- [44] M. Slater, M. Usoh, and A. Steed. Depth of presence in virtual environments. *Presence: Teleoperators and Virtual Environments*, 3(2):130–144, 1994. doi: 10.1162/pres.1994.3.2.130
- [45] J. Spillmann, S. Tuchschnid, and M. Harders. Adaptive space warping to enhance passive haptics in an arthroscopy surgical simulator. *IEEE Transactions on Visualization and Computer Graphics*, 19(4):626–633, 2013. doi: 10.1109/TVCG.2013.23
- [46] F. Steinicke, G. Bruder, K. Hinrichs, and P. Willemsen. Change blindness phenomena for stereoscopic projection systems. In *Proc. VR*, pp. 187–194. IEEE, 2010. doi: 10.1109/VR.2010.5444790
- [47] P. L. Strandholt, O. A. Dogaru, N. C. Nilsson, R. Nordahl, and S. Serafin. Knock on wood: Combining redirected touching and physical props for tool-based interaction in virtual reality. In *Proc. CHI*, pp. 1—13. ACM, New York, NY, USA, 2020. doi: 10.1145/3313831.3376303
- [48] E. A. Suma, S. Clark, S. L. Finkelstein, and Z. Wartell. Exploiting change blindness to expand walkable space in a virtual environment. In *Proc. VR*, pp. 305–306. IEEE, 2010. doi: 10.1109/VR.2010.5444752
- [49] E. A. Suma, S. Clark, D. Krum, S. Finkelstein, M. Bolas, and Z. Wartel. Leveraging change blindness for redirection in virtual environments. In *Proc. VR*, pp. 159–166. IEEE, 2011. doi: 10.1109/VR.2011.5759455
- [50] E. A. Suma, Z. Lipps, S. Finkelstein, D. M. Krum, and M. Bolas. Impossible spaces: Maximizing natural walking in virtual environments with self-overlapping architecture. *IEEE Transactions on Visualization and Computer Graphics*, 18(4):555–564, 2012. doi: 10.1109/TVCG.2012.47
- [51] Q. Sun, A. Patney, L.-Y. Wei, O. Shapira, J. Lu, P. Asente, S. Zhu, M. Mcguire, D. Luebke, and A. Kaufman. Towards virtual reality infinite walking: Dynamic saccadic redirection. *ACM Trans. Graph.*, 37(4), July 2018. doi: 10.1145/3197517.3201294
- [52] R. J. van Beers, D. M. Wolpert, and P. Haggard. When feeling is more important than seeing in sensorimotor adaptation. *Current Biology*, 12(10):834 – 837, 2002. doi: 10.1016/S0960-9822(02)00836-9
- [53] F. VanderWerf, P. Brassinga, D. Reits, M. Aramideh, and B. Ongerboer de Visser. Eyelid movements: Behavioral studies of blinking in humans under different stimulus conditions. *Journal of Neurophysiology*, 89(5):2784–2796, 2003. PMID: 12612018. doi: 10.1152/jn.00557.2002
- [54] F. C. Volkman. Human visual suppression. *Vision Research*, 26(9):1401–1416, 1986. Twenty-Fifth Anniversary Issue of Vision Research. doi: 10.1016/0042-6989(86)90164-1
- [55] E. J. Williams. Experimental designs balanced for the estimation of residual effects of treatments. *Australian Journal of Chemistry*, 2(2):149–168, 1949. doi: 10.1071/CH9490149
- [56] J. J. Yang, H. Horii, A. Thayer, and R. Ballagas. VR Grabbers: Un-grounded haptic retargeting for precision grabbing tools. In *Proc. UIST*, pp. 889—899. ACM, New York, NY, USA, 2018. doi: 10.1145/3242587.3242643
- [57] A. Zenner and A. Krüger. Shifty: A weight-shifting dynamic passive haptic proxy to enhance object perception in virtual reality. *IEEE Transactions on Visualization and Computer Graphics*, 23(4):1285–1294, 2017. doi: 10.1109/TVCG.2017.2656978
- [58] A. Zenner and A. Krüger. Estimating detection thresholds for desktop-scale hand redirection in virtual reality. In *Proc. VR*, pp. 47–55. IEEE, March 2019. doi: 10.1109/VR.2019.8798143
- [59] A. Zenner and A. Krüger. Shifting & Warping: A case for the combined use of dynamic passive haptics and haptic retargeting in VR. In *Adjunct Proc. UIST*. ACM, 2020. doi: 10.1145/3379350.3416166
- [60] Y. Zhao and S. Follmer. A functional optimization based approach for continuous 3D retargeted touch of arbitrary, complex boundaries in haptic virtual reality. In *Proc. CHI*, pp. 544:1–544:12. ACM, New York, NY, USA, 2018. doi: 10.1145/3173574.3174118